Transient Heat Transfer Flow along a Vertical Plate with Induced Magnetic Field

Md. Asaduzzaman[1], Md. Rafiqul Islam[2*] and Ariful Islam[3]

[1]Deptartment of Computer Science & Engineering, North Western University, Khulna-9001, Bangladesh.
[2]Deptartment of Mathematics, Pabna University of Science & Technology,
Pabna-6600, Bangladesh.
[3] Mathematics Discipline, Khulna University, Khulna-9208, Bangladesh.

[*]Email: rafiqku.islam@gmail.com

Abstract- In the field of geophysical and astrophysical engineering, the thermal instability in nature, in chemical processes, in separation processes and in industrial applications the effect of thermal diffusion on the MHD heat transfer in an unsteady flow past through vertical plate is very much important. It has been investigated numerically under the action of a strong applied magnetic field taking into account the induced magnetic field. This study is performed for cooling problem with lighter and heavier particles. Numerical solutions for the velocity field, induced magnetic field and temperature distribution are obtained for associated parameters using the explicit finite difference method. The obtained results are discussed with the help of graphs using Fortran programming as well as Techplot to observe the effects of various parameters on the above mentioned quantities.Finally, the important findings of the investigation are concluded.

Keywords- Transient heat, Magnetic Diffusivity, induced magnetic field, thermal diffusion, viscous dissipation

1 Introduction:

Heat transfer plays an important role in fluids condensing or boiling at a solid surface. The heat transfer consideration arises due to buoyancy forces caused by thermal diffusions. Condensing and boiling are characteristic for many separation processes in chemical engineering as drying, evaporation, distillation, condensation, rectification and absorption of a fluid. [5] *Pera* and *Gebhart*(1971) was first author to investigate the combined buoyancy effects of thermal and mass diffusions on natural convection flow. [9] *Lin* and *Wu*(1997) have studied simultaneous heat and mass transfer model with the entire range of buoyancy ratio for most practical chemical species in dilute and aqueous solutions. [4] *Chen*(2004) have observed the MHD combined heat and mass transfer in natural convection adjacent to a vertical surface.

Along with these studies, the effect of thermal diffusion on MHD free convection and mass transfer flows have also been considered by many investigators due to its important role particularly in isotope separation and in mixtures between gases with very light molecular weight (H_2, H_e) and medium molecular weight (N_2, air) (*Eckert* and *Drake,* 1972). Recently, [11] *Alam et al*.(2006) have numerically investigated the mass transfer flow past a vertical porous medium with heat generation and thermal diffusion on the combined free-forced convection under the influence of transversely applied magnetic field.

In all the papers cited earlier, the studies concentrated on MHD free convection and mass transfer flow of an incompressible viscous fluid past a continuously moving surface under only the action of transverse magnetic field with or without thermal diffusion. But the flow under the action of a strong magnetic field that induced another magnetic field have of great interest in geophysics and astrophysics. [3] *Chaudhary* and *Sharma*(2006) have analytically analyzed the steady combined heat and mass transfer flow with induced magnetic field. There are analytical solution restrictions in their studies. Quite recently, a numerical study of steady combined heat and mass transfer by mixed convection flow past a continuously moving infinite vertical porous plate under the action of strong magnetic field with constant suction velocity, constant heat and mass fluxes have been investigated by [11] *Alam et. al*.(2008). For unsteady two dimensional case, the above problem becomes more complicated. These type of problems play a special role in nature, in many separation processes as isotope separation, in mixtures between gases, in many industrial applications as solidification of binary alloy as well as in astrophysical and geophysical engineering.

2 Mathematical Model

A flow model of transient MHD heat transfer of an electrically conducting incompressible viscous fluid past an electrically non-conducting continuously moving semi-infinite vertical plate with thermal diffusion is considered. Introducing the Cartesian coordinate system, the *x*-axis is

chosen along the porous plate in the direction of flow and the *y*-axis is normal to it. A strong uniform magnetic field is applied normal to the flow region. Because of the magnetic Reynolds number the flow is not taken to be small enough, the induced magnetic field is not negligible. The induced magnetic field is of the form $(H_x, H_y, 0)$. The divergence

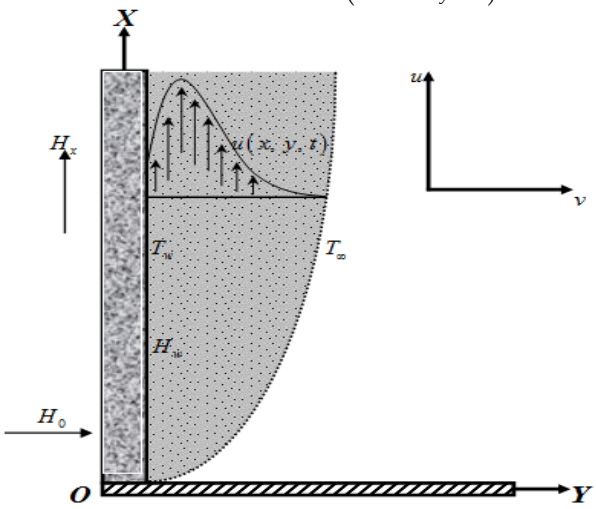

Fig.1 Physical configuration and coordinate system.

equation $\nabla.\mathbf{H} = 0$ of Maxwell's equation for the magnetic field gives $H_y = H_0$.

Initially we consider that the plate as well as the fluid are at the same temperature $T(=T_\infty)$ everywhere in the fluid is same. Also it is assumed that the fluid and the plate is at rest after that the plate is to be moving with a constant velocity U_0 in its own plane and instantaneously at time $t > 0$, the temperature of the plate is raised to $T_w(>T_\infty)$, which is thereafter maintained constant, where T_w is the temperature at the wall and T_∞ is the temperature of the species far away from the plate respectively.

The physical model of this study is furnished in the following figure.

Also the analysis is based on the following assumptions:

i. All the physical properties of the fluid are considered to be constant except the influence of variations of density with temperature are considered only on the body force term, in accordance with the Boussinesq's approximation.

ii. There is no chemical reaction taking place between the foreign mass and the fluid.

iii.The equation of conservation of electric charge, $\nabla.\mathbf{J} = 0$ gives $J_y = $ constant where the current density $\mathbf{J} = (J_x, J_y, J_z)$, because the direction of propagation is considered only along the *y*-axis and $\mathbf{J}$ does not have any variation along the *y*-axis. Since the plate is electrically non-conducting, the constant is zero i.e. $J_y = 0$ at the plate and everywhere.

Continuity equation

$$\frac{\partial u}{\partial x} + \frac{\partial v}{\partial y} = 0 \tag{1}$$

Momentum equation

$$\frac{\partial u}{\partial t} + u\frac{\partial u}{\partial x} + v\frac{\partial u}{\partial y} = g\beta(T - T_\infty) + \upsilon\frac{\partial^2 u}{\partial y^2} + \frac{\mu_e}{\rho}H_0\frac{\partial H_x}{\partial y} + \frac{\upsilon}{k'}u \tag{2}$$

Magnetic induction equation

$$\frac{\partial H_x}{\partial t} + u\frac{\partial H_x}{\partial x} + v\frac{\partial H_x}{\partial y} = H_x\frac{\partial u}{\partial x} + H_0\frac{\partial u}{\partial y} + \frac{1}{\sigma\mu_e}\frac{\partial^2 H_x}{\partial y^2} \tag{3}$$

Energy equation

$$\frac{\partial T}{\partial t} + u\frac{\partial T}{\partial x} + v\frac{\partial T}{\partial y} = \frac{\kappa}{\rho c_p}\frac{\partial^2 T}{\partial y^2} + \frac{1}{\rho c_p \sigma}\left(\frac{\partial H_x}{\partial y}\right)^2 + \frac{\upsilon}{c_p}\left(\frac{\partial u}{\partial y}\right)^2 \tag{4}$$

with the corresponding initial and boundary conditions are

$$t = 0, \quad u = 0, \quad v = 0, \quad H_x = 0, \quad T \to T_\infty \quad \text{everywhere} \tag{5}$$

$$t > 0, \quad u = 0, \quad v = 0, \quad H_x = 0, \quad T \to T_\infty \quad \text{at } x = 0$$

$$u = 0, \quad v = 0, \quad H_x = H_w, \quad T = T_w \quad \text{at } y = 0$$

$$u = 0, \quad v = 0, \quad H_x = 0, \quad T \to T_\infty \quad \text{as } y \to \infty \tag{6}$$

where x, y are Cartesian coordinate system; u, v are x, y component of flow velocity respectively; g is the local acceleration due to gravity; β is the thermal expansion coefficient; υ is the kinematic viscosity; μ_e is the magnetic permeability; ρ is the density of the fluid; H_0 is the constant induced magnetic field; H_x be the x-component induced magnetic field; σ is the electrical conductivity; κ is the thermal conductivity; c_p is the specific heat at the constant pressure and H_w is the induced magnetic field at the wall.

1 Mathematical Formulation

Since the solutions of the governing equations (1) to (4) under the initial (5) and boundary (6) conditions will be based on the finite difference method it is required to make the said equations dimensionless. For this purpose we now introduce the following dimensionless quantities;

$$X = \frac{xU_0}{\upsilon}, Y = \frac{yU_0}{\upsilon}, \quad U = \frac{u}{U_0}, V = \frac{v}{U_0}, \tau = \frac{tU_0^2}{\upsilon},$$

$$\bar{H}_x = \sqrt{\frac{\mu_e}{\rho}}\frac{H_x}{U_0}, \text{ And } \bar{T} = \frac{T - T_\infty}{T_w - T_\infty}$$

From the above dimensionless variable we have

$u = U_0 U$, $v = U_0 V$, $H_x = U_0 \sqrt{\frac{\rho}{\mu_e}} \bar{H}_x$, and

$T = T_\infty + (T_w - T_\infty)\bar{T}$.

Using these relations we have the following derivatives

$$\frac{\partial u}{\partial t} = \frac{U_0^3}{\upsilon}\frac{\partial U}{\partial \tau}, \quad \frac{\partial u}{\partial x} = \frac{U_0^2}{\upsilon}\frac{\partial U}{\partial X}, \quad \frac{\partial u}{\partial y} = \frac{U_0^2}{\upsilon}\frac{\partial U}{\partial Y},$$

$$\frac{\partial^2 u}{\partial y^2} = \frac{U_0^3}{\upsilon^2}\frac{\partial^2 U}{\partial Y^2}, \quad \frac{\partial v}{\partial y} = \frac{U_0^2}{\upsilon}\frac{\partial V}{\partial Y}, \quad \frac{\partial H_x}{\partial t} = \frac{U_0^3}{\upsilon}\sqrt{\frac{\rho}{\mu_e}}\frac{\partial \bar{H}_x}{\partial \tau},$$

$$\frac{\partial H_x}{\partial x} = \frac{U_0^2}{\upsilon}\sqrt{\frac{\rho}{\mu_e}}\frac{\partial \bar{H}_x}{\partial X}, \quad \frac{\partial H_x}{\partial y} = \frac{U_0^2}{\upsilon}\sqrt{\frac{\rho}{\mu_e}}\frac{\partial \bar{H}_x}{\partial Y},$$

$$\frac{\partial^2 H_x}{\partial y^2} = \frac{U_0^3}{\upsilon^2}\sqrt{\frac{\rho}{\mu_e}}\frac{\partial^2 \bar{H}_x}{\partial Y^2}, \quad \frac{\partial T}{\partial t} = \frac{U_0^2 (T_w - T_\infty)}{\upsilon}\frac{\partial \bar{T}}{\partial \tau},$$

$$\frac{\partial T}{\partial x} = \frac{U_0 (T_w - T_\infty)}{\upsilon}\frac{\partial \bar{T}}{\partial X}, \quad \frac{\partial T}{\partial y} = \frac{U_0 (T_w - T_\infty)}{\upsilon}\frac{\partial \bar{T}}{\partial Y},$$

$$\frac{\partial^2 T}{\partial y^2} = \frac{U_0^2 (T_w - T_\infty)}{\upsilon^2}\frac{\partial^2 \bar{T}}{\partial Y^2}.$$

Now we substitute the values of the above derivatives into the equations (1) to (4) and after simplification we obtain the following nonlinear coupled partial differential equations interms of dimensionless variables

$$\frac{\partial U}{\partial X} + \frac{\partial V}{\partial Y} = 0 \qquad (7)$$

$$\frac{\partial U}{\partial \tau} + U\frac{\partial U}{\partial X} + V\frac{\partial U}{\partial Y} = G_r \bar{T} + \frac{\partial^2 U}{\partial Y^2} + M\frac{\partial \bar{H}_x}{\partial Y} + \kappa U \qquad (8)$$

$$\frac{\partial \bar{H}_x}{\partial \tau} + U\frac{\partial \bar{H}_x}{\partial X} + V\frac{\partial \bar{H}_x}{\partial Y} = \bar{H}_x\frac{\partial U}{\partial X} + M\frac{\partial U}{\partial Y} + \frac{1}{P_m}\frac{\partial^2 \bar{H}_x}{\partial Y^2} \qquad (9)$$

$$\frac{\partial \bar{T}}{\partial \tau} + U\frac{\partial \bar{T}}{\partial X} + V\frac{\partial \bar{T}}{\partial Y} = \frac{1}{P_r}\frac{\partial^2 \bar{T}}{\partial Y^2} + \frac{E_c}{P_m}\left(\frac{\partial \bar{H}_x}{\partial Y}\right)^2 + E_c\left(\frac{\partial U}{\partial Y}\right)^2 \qquad (10)$$

where $G_r = \frac{\upsilon g \beta (T_w - T_\infty)}{U_0^3}$ (**Grashof Number**),

$M = \frac{H_0}{U_0}\sqrt{\frac{\mu_e}{\rho}}$ (**Magnetic Force Number**),

$P_m = \upsilon \sigma' \mu_e$ (**Magnetic diffusivity Number**),

$P_r = \frac{\upsilon \rho c_p}{\kappa}$ (**Prandtl Number**),

$E_c = \frac{U_0^2}{c_p (T_w - T_\infty)}$ (**Eckert Number**) and

$\kappa = \frac{\upsilon^2}{\kappa' U_0^2}$

Also the associated initial (5) and boundary (6) conditions become

$$\tau = 0, \quad U = 0, \quad V = 0, \quad \bar{H}_x = 0, \quad \bar{T} = 0 \text{ everywhere} \qquad (11)$$

$$\tau > 0, \quad U = 0, \quad V = 0, \quad \bar{H}_x = 0, \quad \bar{T} = 0 \text{ at } X = 0$$

$$U = 0, \quad V = 0, \quad \bar{H}_x = 1, \quad \bar{T} = 1 \text{ at } Y = 0$$

$$U = 0, \quad V = 0, \quad \bar{H}_x = 0, \quad \bar{T} = 0 \text{ as } Y \to \infty \qquad (12)$$

1 Numerical Solutions

The explicit finite difference method has been used to solve equations (7) to (10) subject to the conditions given by (11) and (12). To obtain the difference equations the region of the flow is divided into a grid or mesh of lines parallel to *X* and *Y* axes where *X*-axis is taken along the plate and *Y*-axis is normal to the plate.

Here we consider that the plate of height $X_{\max}(=100)$ i.e. *X* varies from 0 to 100 and regard $Y_{\max}(=25)$ as corresponding to $Y \to \infty$ i.e. *Y* varies from 0 to 25. There are $m = 125$ and $n = 125$ grid spacing in the *X* and *Y* directions respectively as

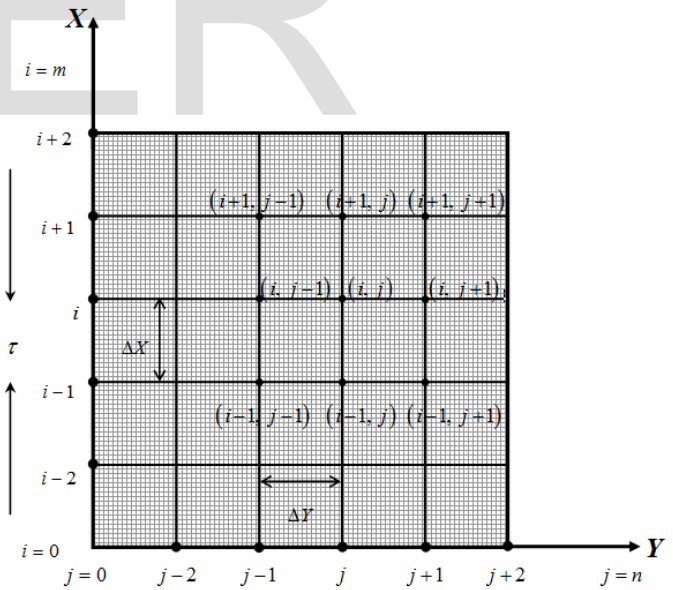

Fig. 2 Finite difference space grid.

shown in **Fig.2.**

It is assumed that ΔX , ΔY are constant mesh sizes along *X* and *Y* directions respectively and taken as follows,

$$\Delta X = 0.8(0 \le x \le 100)$$

$$\Delta Y = 0.2(0 \le y \le 25)$$

with the smaller time-step, $\Delta \tau = 0.005$

Let U', V', $\bar{H}_x'$ and $\bar{T}'$ denote the values of U, V, $\bar{H}_x$ and $\bar{T}$ at the end of a time-step respectively. Using the explicit finite difference approximation we have,

$$\left(\frac{\partial U}{\partial \tau}\right)_{i,j} = \frac{U'_{i,j} - U_{i,j}}{\Delta\tau}, \left(\frac{\partial U}{\partial X}\right)_{i,j} = \frac{U_{i,j} - U_{i-1,j}}{\Delta X},$$

$$\left(\frac{\partial U}{\partial Y}\right)_{i,j} = \frac{U_{i,j+1} - U_{i,j}}{\Delta Y},$$

$$\left(\frac{\partial V}{\partial Y}\right)_{i,j} = \frac{V_{i,j} - V_{i,j-1}}{\Delta Y}, \left(\frac{\partial \bar{H}_x}{\partial \tau}\right)_{i,j} = \frac{\bar{H}'_{x\,i,j} - \bar{H}_{x\,i,j}}{\Delta\tau},$$

$$\left(\frac{\partial \bar{H}_x}{\partial X}\right)_{i,j} = \frac{\bar{H}_{x\,i,j} - \bar{H}_{x\,i-1,j}}{\Delta X},$$

$$\left(\frac{\partial \bar{H}_x}{\partial Y}\right)_{i,j} = \frac{\bar{H}_{x\,i,j+1} - \bar{H}_{x\,i,j}}{\Delta Y}, \quad \left(\frac{\partial \bar{T}}{\partial \tau}\right)_{i,j} = \frac{\bar{T}'_{i,j} - \bar{T}_{i,j}}{\Delta\tau},$$

$$\left(\frac{\partial \bar{T}}{\partial X}\right)_{i,j} = \frac{\bar{T}_{i,j} - \bar{T}_{i-1,j}}{\Delta X}, \left(\frac{\partial \bar{T}}{\partial Y}\right)_{i,j} = \frac{\bar{T}_{i,j+1} - \bar{T}_{i,j}}{\Delta Y},$$

$$\left(\frac{\partial^2 U}{\partial Y^2}\right)_{i,j} = \frac{U_{i,j+1} - 2U_{i,j} + U_{i,j-1}}{(\Delta Y)^2},$$

$$\left(\frac{\partial^2 \bar{H}_x}{\partial Y^2}\right)_{i,j} = \frac{\bar{H}_{x\,i,j+1} - 2\bar{H}_{x\,i,j} + \bar{H}_{x\,i,j-1}}{(\Delta Y)^2} \text{ and}$$

$$\left(\frac{\partial^2 \bar{T}}{\partial Y^2}\right)_{i,j} = \frac{\bar{T}_{i,j+1} - 2\bar{T}_{i,j} + \bar{T}_{i,j-1}}{(\Delta Y)^2}.$$

From the system of partial differential equations (7) to (10) with substituting the above relations into the corresponding differential equation we obtain an appropriate set of finite difference equations,

$$\frac{U'_{i,j} - U'_{i-1,j}}{\Delta X} + \frac{V_{i,j} - V_{i,j-1}}{\Delta Y} = 0 \tag{13}$$

$$\frac{U'_{i,j} - U_{i,j}}{\Delta\tau} + U_{i,j}\frac{U_{i,j} - U_{i-1,j}}{\Delta X} + V_{i,j}\frac{U_{i,j+1} - U_{i,j}}{\Delta Y} = G_r \bar{T}'_{i,j}$$
$$+ \frac{U_{i,j+1} - 2U_{i,j} + U_{i,j-1}}{(\Delta Y)^2} + M\frac{\bar{H}_{x\,i,j+1} - \bar{H}_{x\,i,j}}{\Delta Y} + \kappa U_{i,j} \tag{14}$$

$$\frac{\bar{H}'_{x\,i,j} - \bar{H}_{x\,i,j}}{\Delta\tau} + U_{i,j}\frac{\bar{H}_{x\,i,j} - \bar{H}_{x\,i-1,j}}{\Delta X} + V_{i,j}\frac{\bar{H}_{x\,i,j+1} - \bar{H}_{x\,i,j}}{\Delta Y} = \bar{H}_{x\,i,j}\frac{U_{i,j} - U_{i-1,j}}{\Delta X}$$
$$+ M\frac{U_{i,j+1} - U_{i,j}}{\Delta Y} + \frac{1}{P_m}\frac{\bar{H}_{x\,i,j+1} - 2\bar{H}_{x\,i,j} + \bar{H}_{x\,i,j-1}}{(\Delta Y)^2} \tag{15}$$

$$\frac{\bar{T}'_{i,j} - \bar{T}_{i,j}}{\Delta\tau} + U_{i,j}\frac{\bar{T}_{i,j} - \bar{T}_{i-1,j}}{\Delta X} + V_{i,j}\frac{\bar{T}_{i,j+1} - \bar{T}_{i,j}}{\Delta Y} = \frac{1}{P_r}\frac{\bar{T}_{i,j+1} - 2\bar{T}_{i,j} + \bar{T}_{i,j-1}}{(\Delta Y)^2}$$
$$+ \frac{E_c}{P_m}\left(\frac{\bar{H}_{x\,i,j+1} - \bar{H}_{x\,i,j}}{\Delta Y}\right)^2 + E_c\left(\frac{U_{i,j+1} - U_{i,j}}{\Delta Y}\right)^2 \tag{16}$$

and the initial and boundary conditions with the finite difference scheme are

$$U^0_{i,j} = 0, \quad V^0_{i,j} = 0, \quad \bar{H}^0_{x\,i,j} = 0, \quad \bar{T}^0_{i,j} = 0 \tag{17}$$

$$U^n_{0,j} = 0, \quad V^n_{0,j} = 0, \quad \bar{H}^n_{x\,0,j} = 0, \quad \bar{T}^0_{0,j} = 0$$
$$U^n_{i,0} = 0, \quad V^n_{i,0} = 0, \quad \bar{H}^n_{x\,i,0} = 1, \quad \bar{T}^n_{i,0} = 1$$
$$U^n_{i,L} = 0, \quad V^n_{i,L} = 0, \quad \bar{H}^n_{x\,i,L} = 0, \quad \bar{T}^n_{i,L} = 0$$

where $L \to \infty$. (18)

Here the subscripts i and j designate the grid points with x and y coordinates respectively and the superscript n represents a value of time, $\tau = n\Delta\tau$ where $n = 0, 1, 2, \ldots$. From the initial condition (17), the values of U, $\bar{H}_x$ and $\bar{T}$ are known at $\tau = 0$. During any one time-step, the coefficients $U_{i,j}$ and $V_{i,j}$ appearing in equations (14) to (16) are treated as constants. Then at the end of any time-step $\Delta\tau$, the new temperature $\bar{T}'$, the new velocity U', the new induced magnetic field $\bar{H}_x'$ and V' at all interior nodal points may be obtained by successive applications of equations (16), (14), (15) and (13) respectively. This process is repeated in time and provided the time-step is sufficiently small, U, V, $\bar{H}_x$ and $\bar{T}$ should eventually converge to values which approximate the steady-state solution of equations (7) to (10). These converged solutions are shown graphically in Figs. 3 to 38.

For the purpose of discussing the results of the problem, the approximate solutions are obtained for various parameters with small values of Eckert number. In order to analyze the physical situation of the model, we have computed the steady state numerical values of the non-dimensional velocity U, induced magnetic field $\bar{H}_x$ and temperature $\bar{T}$ within the boundary layer for different values of magnetic parameter (M), magnetic diffusivity (P_m), Grashof number (G_r), Prandtl number (P_r) and Eckert number (E_c).

To get the steady state solutions, the computations have been carried out upto $\tau = 80$. We observed that the results of the computations, however, show no visible changes after $\tau = 40$. Thus the solution for $\tau = 40$ are essentially steady state solutions.

Because of the special importance of cooling problem in nuclear engineering in connection with the cooling of reactors, the value of the Grashof number for heat transfer is taken to be positive $(G_r > 0)$ and the present study has considered $G_r = 1.0$, 1.2 and 1.4. Since the most important fluids are atmospheric air, salt water and water so the results are limited to $P_r = 0.71$ (Prandtl number for air at 20°C), $P_r = 1.0$ (Prandtl number for salt water at 20°C) and $P_r = 7.0$ (Prandtl number for water at 20°C). However the values of another parameters M, P_m and E_c are chosen arbitrarily as M = 0.10, 0.20 and 0.30; P_m =1.0, 1.5 and 2.0; E_c =0.01, 0.02 and 0.03.

Along with the obtained steady state solutions, the flow behaviors in case of cooling problem are discussed graphically. The profiles of the transient velocity, induced magnetic field and temperature versus Y are illustrated in **Figs. 3 to 38.**

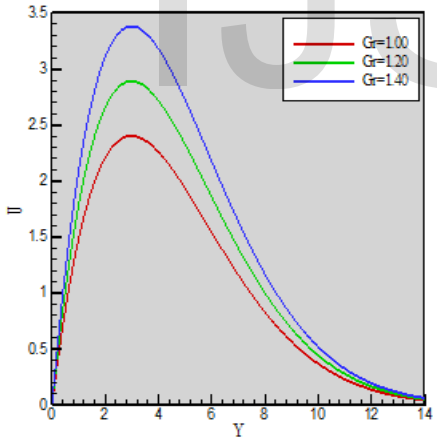

Fig. 3 Velocity profiles for different values of G_r where $M = 0.10$, $P_m = 1.00$, $P_r = 0.71$ and $E_c = 0.01$ at time $\tau = 10$.

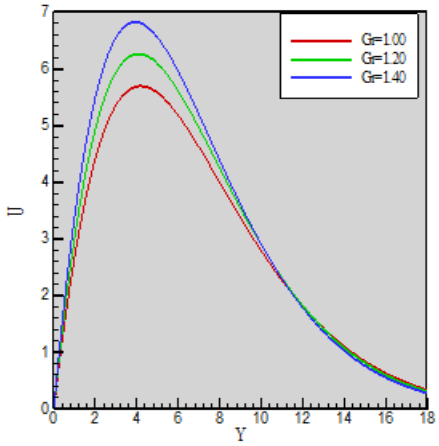

Fig. 4 Velocity profiles for different values of G_r where $M = 0.10$, $P_m = 1.00$, $P_r = 0.71$ and $E_c = 0.01$ at time $\tau = 30$.

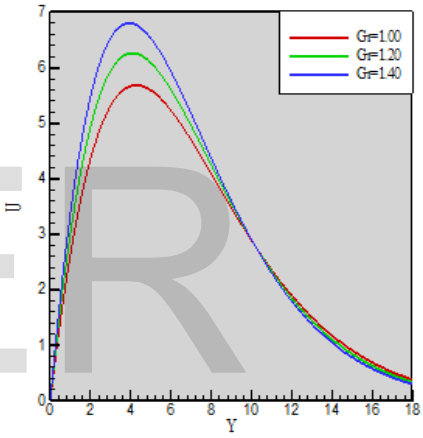

Fig. 5 Velocity profiles for different values of G_r where $M = 0.10$, $P_m = 1.00$, $P_r = 0.71$ and $E_c = 0.01$ at time $\tau = 40$.

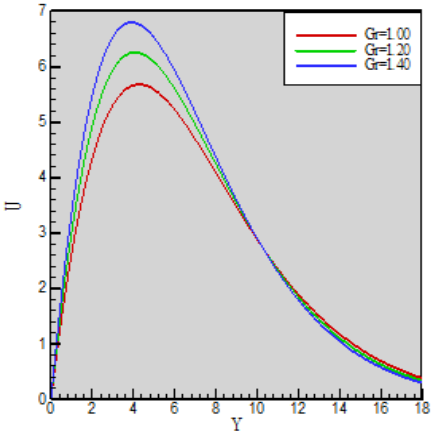

Fig. 6 Velocity profiles for different values of G_r where $M = 0.10$, $P_m = 1.00$, $P_r = 0.71$ and $E_c = 0.01$ at time $\tau = 50$.

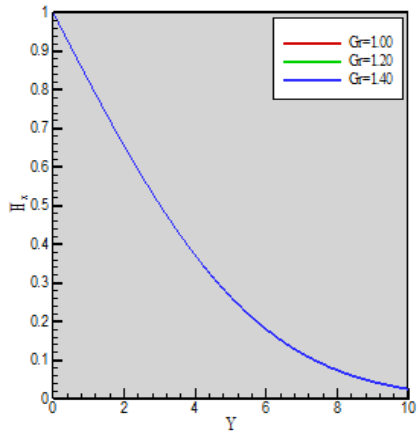

Fig. 7 Induced magnetic fields for different values of G_r where $M = 0.10$, $P_m = 1.00$, $P_r = 0.71$ and $E_c = 0.01$ at time $\tau = 10$.

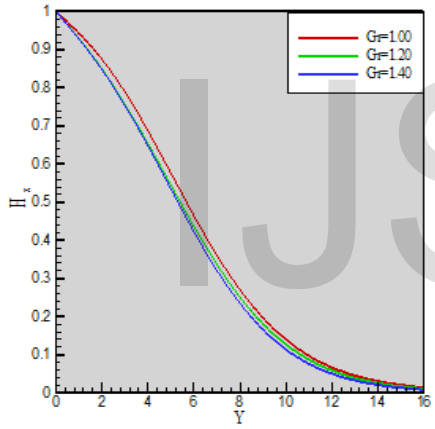

Fig. 8 Induced magnetic fields for different values of G_r where $M = 0.10$, $P_m = 1.00$, $P_r = 0.71$ and $E_c = 0.01$ at time $\tau = 30$.

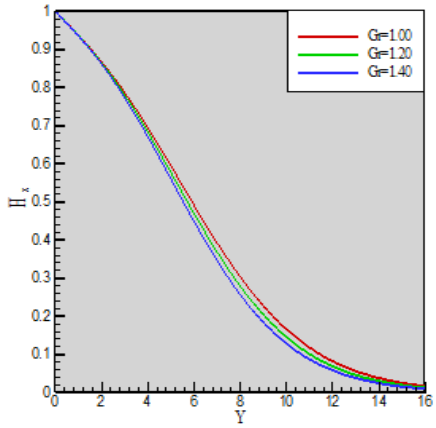

Fig. 9 Induced magnetic fields for different values of G_r where $M = 0.10$, $P_m = 1.00$, $P_r = 0.71$ and $E_c = 0.01$ at time $\tau = 40$.

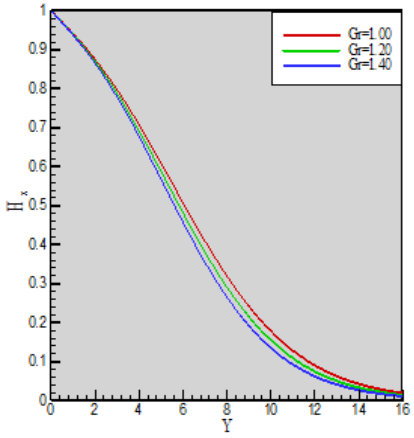

Fig. 10 Induced magnetic fields for different values of G_r where $M = 0.10$, $P_m = 1.00$, $P_r = 0.71$ and $E_c = 0.01$ at time $\tau = 50$.

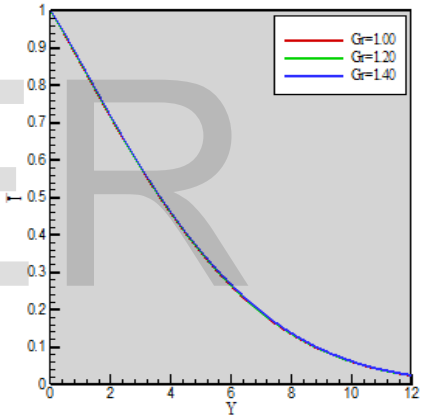

Fig. 11 Temperature profiles for different values of G_r where $M = 0.10$, $P_m = 1.00$, $P_r = 0.71$ and $E_c = 0.01$ at time $\tau = 10$.

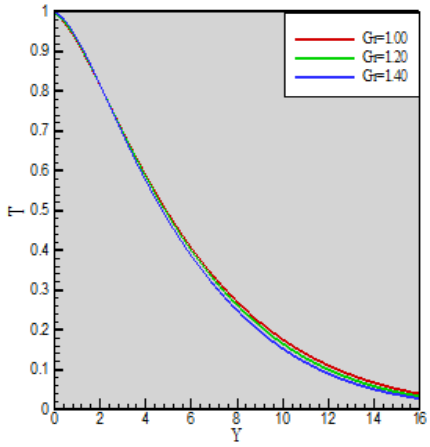

Fig. 12 Temperature profiles for different values of G_r where $M = 0.10$, $P_m = 1.00$, $P_r = 0.71$ and $E_c = 0.01$ at time $\tau = 30$.

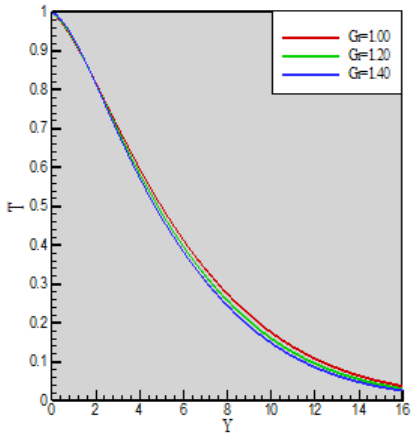

Fig. 13 Temperature profiles for different values of G_r where $M = 0.10$, $P_m = 1.00$, $P_r = 0.71$ and $E_c = 0.01$ at time $\tau = 40$.

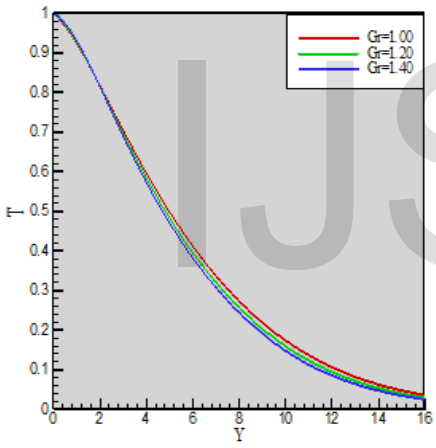

Fig. 14 Temperature profiles for different values of G_r where $M = 0.10$, $P_m = 1.00$, $P_r = 0.71$ and $E_c = 0.01$ at time $\tau = 50$.

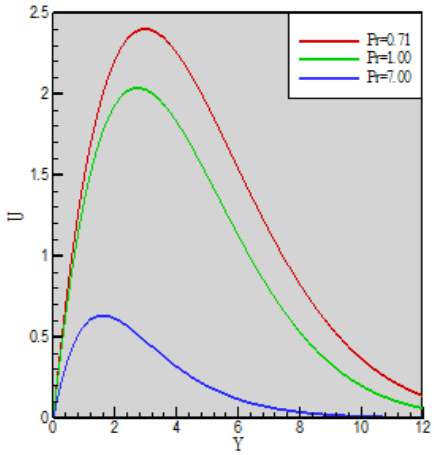

Fig. 15 Velocity profiles for different values of P_r where $G_r = 1.00$, $M = 0.10$, $P_m = 1.00$ and $E_c = 0.01$ at time $\tau = 10$.

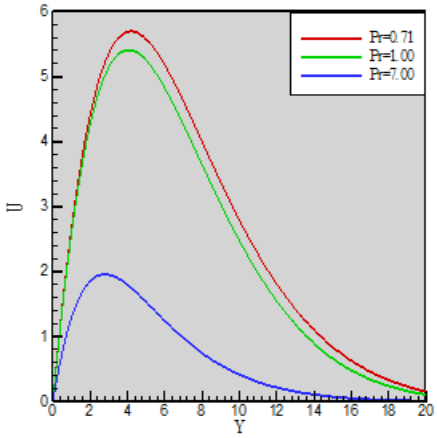

Fig. 16 Velocity profiles for different values of P_r where $G_r = 1.00$, $M = 0.10$, $P_m = 1.00$ and $E_c = 0.01$ at time $\tau = 30$.

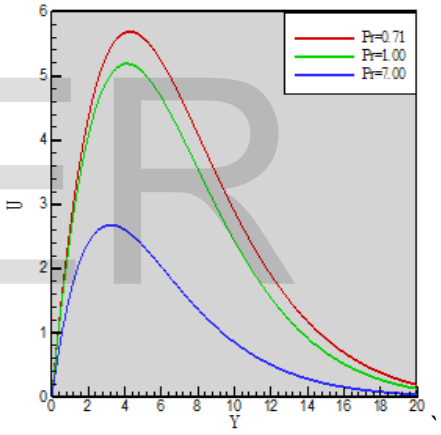

Fig. 17 Velocity profiles for different values of P_r where $G_r = 1.00$, $M = 0.10$, $P_m = 1.00$ and $E_c = 0.01$ at time $\tau = 40$.

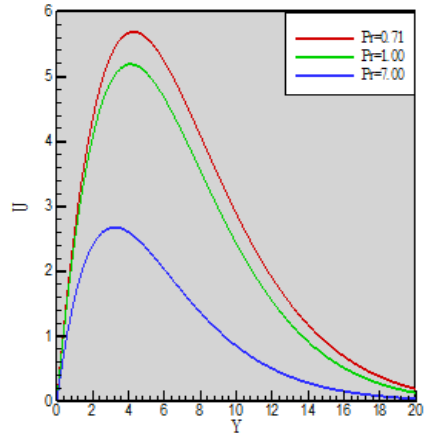

Fig. 18 Velocity profiles for different values of P_r where $G_r = 1.00$, $M = 0.10$, $P_m = 1.00$ and $E_c = 0.01$ at time $\tau = 50$.

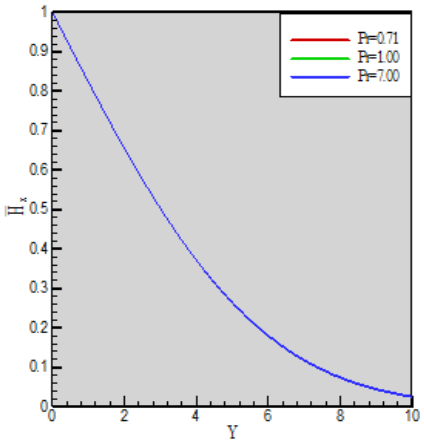

Fig. 19 Induced magnetic fields for different values of P_r where $G_r = 1.00$, $M = 0.10$, $P_m = 1.00$ and $E_c = 0.01$ at time $\tau = 10$.

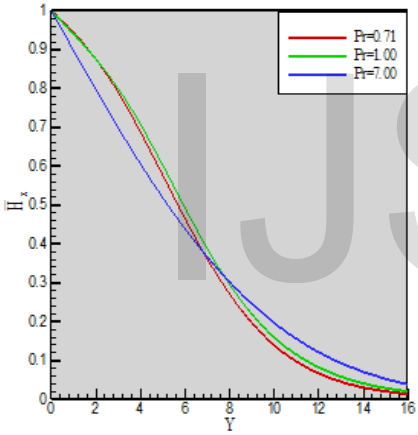

Fig. 20 Induced magnetic fields for different values of P_r where $G_r = 1.00$, $M = 0.10$, $P_m = 1.00$ and $E_c = 0.01$ at time $\tau = 30$.

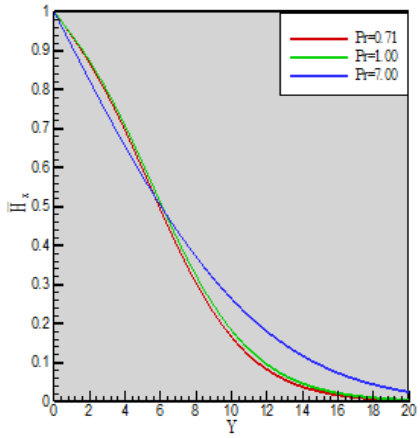

Fig. 21 Induced magnetic fields for different values of P_r where $G_r = 1.00$, $M = 0.10$, $P_m = 1.00$ and $E_c = 0.01$ at time $\tau = 40$.

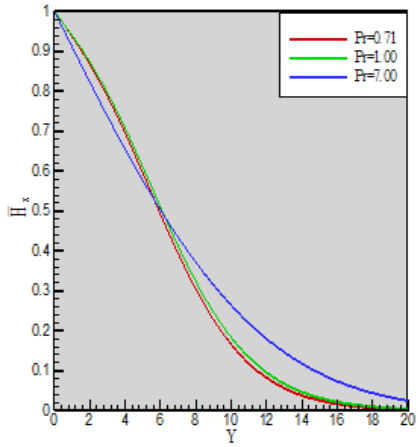

Fig. 22 Induced magnetic fields for different values of P_r where $G_r = 1.00$, $M = 0.10$, $P_m = 1.00$ and $E_c = 0.01$ at time $\tau = 50$.

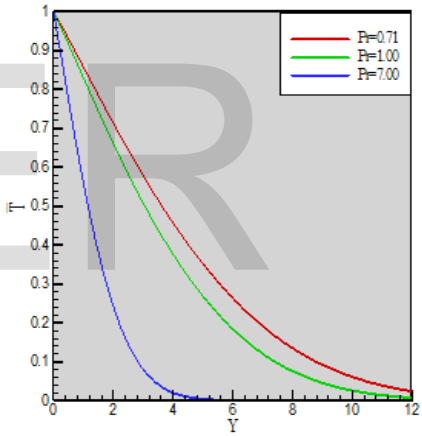

Fig. 23 Temperature profiles for different values of P_r where $G_r = 1.00$, $M = 0.10$, $P_m = 1.00$ and $E_c = 0.01$ at time $\tau = 10$.

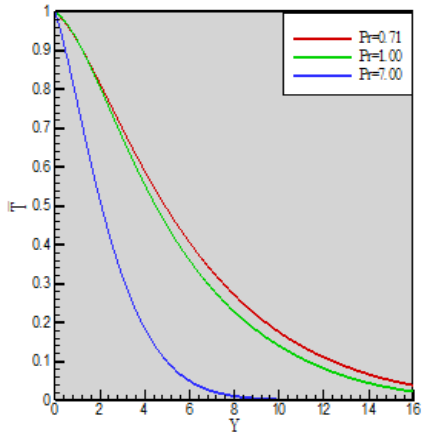

Fig. 24 Temperature profiles for different values of P_r where $G_r = 1.00$, $M = 0.10$, $P_m = 1.00$ and $E_c = 0.01$ at time $\tau = 30$.

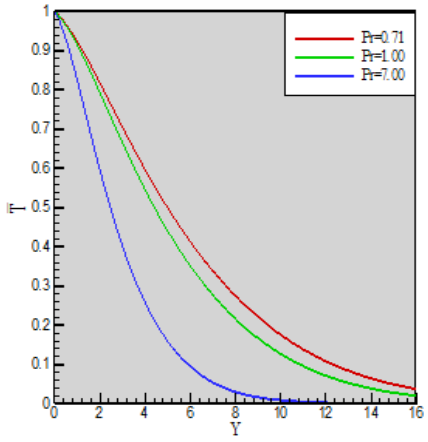

Fig. 25 Temperature profiles for different values of P_r where $G_r = 1.00$, $M = 0.10$, $P_m = 1.00$ and $E_c = 0.01$ at time $\tau = 40$.

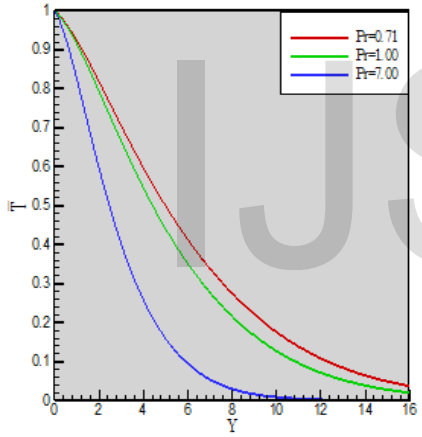

Fig. 26 Temperature profiles for different values of P_r where $G_r = 1.00$, $M = 0.10$, $P_m = 1.00$ and $E_c = 0.01$ at time $\tau = 50$.

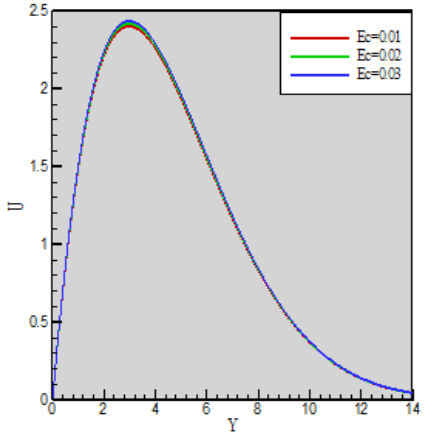

Fig. 27 Velocity profiles for different values of E_c where $G_r = 1.00$, $M = 0.10$, $P_m = 1.00$ and $P_r = 0.71$ at time $\tau = 10$.

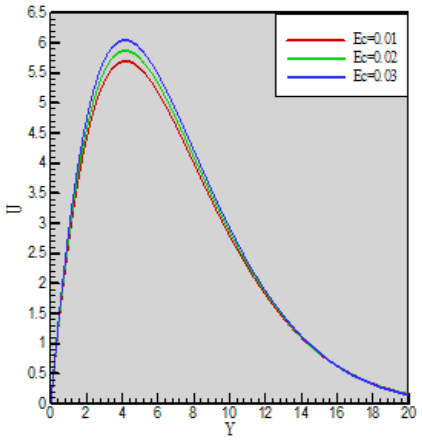

Fig. 28 Velocity profiles for different values of E_c where $G_r = 1.00$, $M = 0.10$, $P_m = 1.00$ and $P_r = 0.71$ at time $\tau = 30$.

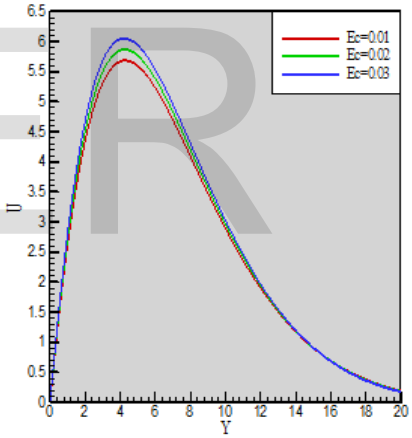

Fig. 29 Velocity profiles for different values of E_c where $G_r = 1.00$, $M = 0.10$, $P_m = 1.00$ and $P_r = 0.71$ at time $\tau = 40$.

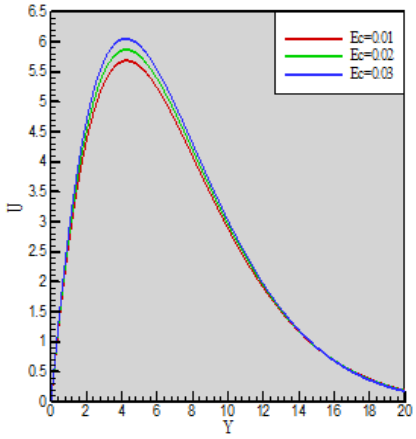

Fig. 30 Velocity profiles for different values of E_c where $G_r = 1.00$, $M = 0.10$, $P_m = 1.00$ and $P_r = 0.71$ at time $\tau = 50$.

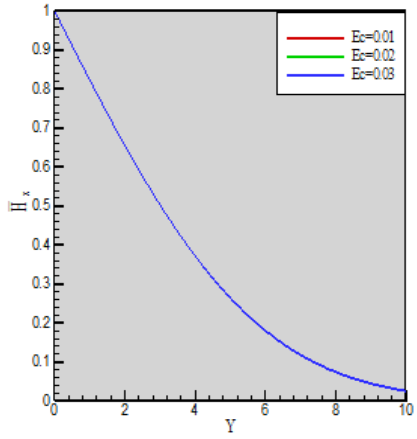

Fig. 31 Induced magnetic fields for different values of E_c where $G_r = 1.00$, $M = 0.10$, $P_m = 1.00$ and $P_r = 0.71$ at time $\tau = 10$.

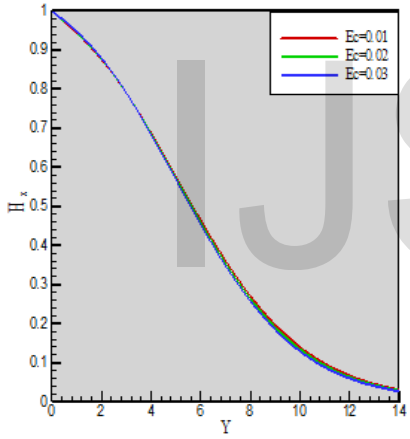

Fig. 32 Induced magnetic fields for different values of E_c where $G_r = 1.00$, $M = 0.10$, $P_m = 1.00$ and $P_r = 0.71$ at time $\tau = 30$.

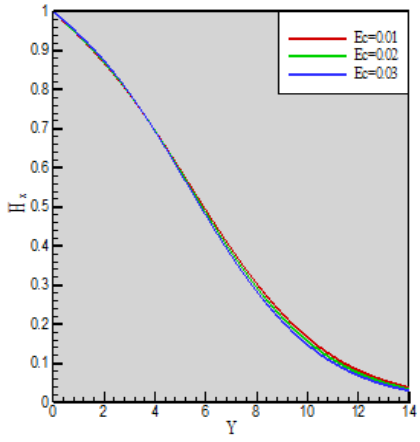

Fig. 33 Induced magnetic fields for different values of E_c where $G_r = 1.00$, $M = 0.10$, $P_m = 1.00$ and $P_r = 0.71$ at time $\tau = 40$.

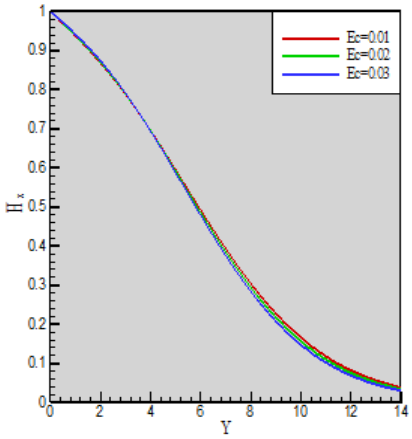

Fig. 34 Induced magnetic fields for different values of E_c where $G_r = 1.00$, $M = 0.10$, $P_m = 1.00$ and $P_r = 0.71$ at time $\tau = 50$.

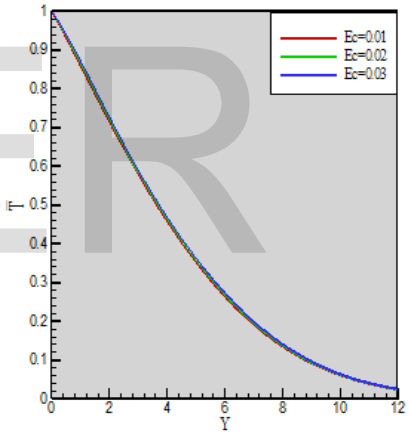

Fig. 35 Temperature profiles for different values of E_c where $G_r = 1.00$, $M = 0.10$, $P_m = 1.00$ and $P_r = 0.71$ at time $\tau = 10$.

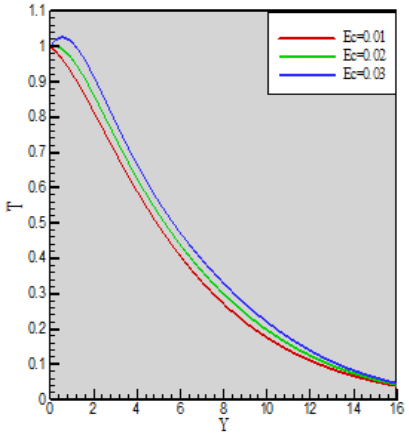

Fig. 36 Temperature profiles for different values of E_c where $G_r = 1.00$, $M = 0.10$, $P_m = 1.00$ and $P_r = 0.71$ at time $\tau = 30$.

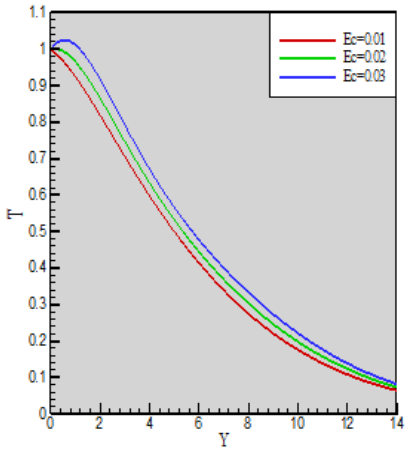

Fig. 37 Temperature profiles for different values of E_c where $G_r = 1.00$, $M = 0.10$, $P_m = 1.00$ and $P_r = 0.71$ at time $\tau = 40$.

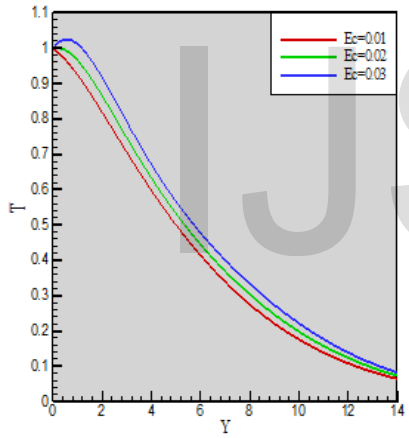

Fig. 38 Temperature profiles for different values of E_c where $G_r = 1.00$, $M = 0.10$, $P_m = 1.00$ and $P_r = 0.71$ at time $\tau = 50$.

For avoiding the complexity here we show the variations for τ =10, 30, 40 and 50. For the change of G_r, the velocity profile is shown in (**Figs. 3 to 6).** From these Fig. we see that, as the value of G_r increases the velocity profile also increases at τ =10, 30 and 40. But at τ =50 the velocity profile shows same graph as τ =40. One the other hand, as the value of τ increases the velocity profiles also increase upto τ =40. But at τ =50 the velocity profile shows same graph as τ =40.
The induced magnetic field profile **(Figs. 7 to 10)** remains same as the value of G_r increases at τ =10. But for τ =30, 40 and 50 the induced magnetic field profile decreases as the value of G_r increases. At τ =50 the induced magnetic field profile shows identical graph as τ =40. Also as the value of τ increases the velocity profiles also increase upto τ =40. But at τ =50 the velocity profile shows same graph as τ =40.
The temperature profile **(Figs. 11 to 14)** remains same as the value of G_r increases at τ =10. But for τ =30, 40 and 50 the temperature profile decreases as the value of G_r increases. At τ =50 the temperature profile shows identical graph as τ =40. Also as the value of τ increases the temperature profiles increase upto τ =40. But at τ =50 the temperature profile shows same graph as τ =40.
As the value of Pr increases the velocity profile **(Figs. 15 to 18)** decreases at τ =10, 30 and 40. But at τ =50 the velocity profile shows same graph as τ =40. One the other hand, as the value of τ increases the velocity profiles also increase upto τ =40. But at τ =50 the velocity profile shows same graph as τ =40.
The induced magnetic field profile **(Figs. 19 to 22)** remains same as the value of Pr increases at τ =10. But for τ =30, 40 and 50 the induced magnetic field profile initially decreases and after certain amount of Y it increases as the value of Pr increases. At τ =50 the induced magnetic field profile shows identical graph as τ =40. Also as the value of τ increases the induced magnetic field profiles also increase upto τ =40. But at τ =50 the induced magnetic field profile shows same graph as τ =40.
As the value of Pr increases the temperature profile **(Figs. 23 to 26)** decreases at τ =10, 30 and 40. But at τ =50 the temperature profile shows same graph as τ =40. One the other hand, as the value of τ increases the temperature profiles also increase upto τ =40. But at τ =50 the temperature profile shows same graph as τ =40.

As the value of E_c increases the velocity profile **(Figs. 27 to 30)** also increases at τ =10, 30 and 40. But at τ =50 the velocity profile shows same graph as τ =40. One the other hand, as the value of τ increases the velocity profiles also increase upto τ =40. But at τ =50 the velocity profile shows same graph as τ =40.

The induced magnetic field profile **(Figs. 31 to 34)** remains same as the value of E_c increases at τ =10. But for τ =30, 40 and 50 the induced magnetic field profile decreases as the value of E_c increases. At τ =50 the induced magnetic field profile shows identical graph as τ =40. Also as the value of τ increases the velocity profiles also increase upto τ =40. But at τ =50 the velocity profile shows same graph as τ =40.
As the value of E_c increases the temperature profile **(Figs. 35 to 38)** increases at τ =10, 30 and 40. But at τ =50 the

temperature profile shows same graph as τ =40. One the other hand, as the value of τ increases the temperature profiles also increase upto τ =40. But at τ =50 the temperature profile shows same graph as τ =40.

2 Conclusions

A transient heat transfer flow through an electrically conducting incompressible viscous fluid past an electrically nonconducting continuously moving semi-infinite vertical plate under the action of strong magnetic field taking into account the induced magnetic field constant heat is investigated in this work. The resulting governing system of dimensionless coupled non-linear partial differential equations are numerically solved by an explicit finite difference method. The results are discussed for different values of important parameters as magnetic parameter, magnetic diffusivity numbers, Grashof number, Prandtal number and Eckert number. Some of the important findings obtained from the graphical representation of the results are listed herewith;

1. The velocity increases with the increase of E_c or G_r while it decreases with the increase of P_r.
2. The magnetic induction decreases with the increase of G_r, E_c. Moreover, the magnetic induction initially decreases and later increases with the increase of P_r. Particularly, the induced magnetic field is greater for heavier than lighter particles.
3. The temperature increases with the increase of E_c while it decreases with the increase of G_r or P_r. Particularly, the fluid temperature is more for air than water and it is less for lighter than heavier particles.

As the basis for many scientific and engineering applications for studying more complex vertical problems involving the flow of electrically conducting fluids, it is hoped that the present investigation of the study of applied physics of flow over a vertical surface can be utilized. In the migration of underground water or oil as well as in the filtration and water purification processes, the findings may be useful for study of movement of oil or gas and water through the reservoir of an oil or gas field. The results of the problem are also of great interest in geophysics and astrophysics in the study of interaction of the geomagnetic field with the fluid in geothermal region.

References

[1] Alfven, *"On the existence of electromagnetic Hydromagnetic waves"*, .Mat,Astro.Fysik.Bd.,V.No.2.P.295 H,1942.

[2] Callahan and Marner ,*"Transient free convection on an sothermal vertical flat plate"*, International Journal of Heat and Mass Transfer, vol. 21, p. 67-69, (1976).

[3] Chaudhary, R. C. and Sharma, B. K.,*"The steady combined heat and mass transfer with induced magnetic field"*, Journal of Applied Physics, v.99, p.034901, (2006).

[4] Chen *"Combined heat and mass transfer in MHD free convection from a vertical surface with Ohmic heating and viscous dissipation"*, International Journal of Engineering and Science, v.42, p.699-713, 2004.

[5] Gebhart, B. and Pera, L., *"Combined buoyancy effects of thermal and mass diffusions on natural convection flow"*, Int. J. Heat Mass Transfer, v.14, p.2026, 1971..

[6] G. Labrosse, *"Free convection of binary liquid with variable Soret coefficient in thermogravitational column: The steady parallel base states"*, Phys. Fluids, v.15, p.2694, 2003.

[7] Gokhale MY, *"Magnetohydrodynamic transient free convection past a semi- infinite vertical plate with constant heat flux"*, Canadian Journal of Physics v.69, p.1451-1453, 1991.

[8] Gribben RJ, "*The hydromagnetic boundary layer in the presence of pressure gradient"*, Proceedings of Royal Society. London A v.287, p.123-141, 1965.

[9] Lin and Wu, *"Combined heat and mass transfer by laminar natural convection from a vertical plate with uniform heat flux and concentration"* Int. J. Heat Mass Transfer, v.32, p. 293-299, 1997.

[10] Michael Faraday, *"Electromagnetic Force Field, Particle/Field Duality"* v.2, p.525-1333, 1832.

[11] M. M. Alam, M. R. Islam, F. Rahman, *"Steady heat and mass transfer by mixed convection flow from a vertical porous plate with induced magnetic field, constant heat and mass fluxes"*, Thammasat Int. J. Sc. Tech. v.13, p.4, 2008.

[12] Muthucumaraswamy R, Ganesan P, "*Flow past an impulsively started vertical plate with variable temperature and mass flux, Heat and Mass transfer"*, v. 34, p. 487- 493, 1999.

[13] Ostrach S, "*An analysis of laminar free convection flow and heat transfer along a flat plate parallel to the direction of the generating body force"*,NACA ReportTR1111,p.63-79, 1953.

[14] Peddiesen J,McNitt R.P., "*Boundary layer theory for a micro polar fluid"*, Recent Advanced Engineering and Science, v.5, p.405, 1970.

[15] R. J. Goldstein and E.M. Sparrow, *"Flow and heat transfer in the boundary layer on a continuous moving surface"*, International Journal of Heat and Mass Transfer, v.10, p.219-235, 1967.

[16] Soundalgekar VM, Ganesan P ,"*Finite–Difference analysis of transient free convection with mass transfer on an isothermal vertical flat plate"*, International Journal of Engineering Science, v.19, p.757-770, 1981.

[17] Takhar HS, Ganesan P, Ekambavahar K, Soundalgekar VM ,"*Transient free convection past a semi-infinite vertical plate with variable surface temperature"*, International

Journal of Numerical Methods in Heat Fluid Flow, v.7, p.280-296, 1997.